European Journal of Pharmaceutics and Biopharmaceutics 70 (2008) 453–461

Contents lists available at ScienceDirect

European Journal of Pharmaceutics and Biopharmaceutics

journal homepage: www.elsevier.com/locate/ejpb

Research paper

Poly(*N*-vinylacetamide) chains enhance lectin-induced biorecognition through the reduction of nonspecific interactions with nontargets

Ken-ichiro Hiwatari [a], Shinji Sakuma [b,*], Kiyoko Iwata [b], Yoshie Masaoka [b], Makoto Kataoka [b], Hiroyuki Tachikawa [a], Yoshikazu Shoji [a], Shinji Yamashita [b]

[a] *Advanced Materials R & D Laboratory, ADEKA Co., Tokyo, Japan*
[b] *Faculty of Pharmaceutical Sciences, Setsunan University, Osaka, Japan*

ARTICLE INFO

Article history:
Received 27 August 2007
Accepted in revised form 3 April 2008
Available online 5 June 2008

Keywords:
Endoscopic imaging agent
Nanomedicine
Colonoscopy
Colorectal cancer
Lectin
Poly (*N*-vinylacetamide)

ABSTRACT

Lectin-immobilized fluorescent nanospheres were designed with the aim of developing a novel endoscopic imaging agent for the detection of early colorectal cancer. Submicron-sized polystyrene nanospheres with surface poly(*N*-vinylacetamide) (PNVA) and poly(methacrylic acid) (PMAA) chains encapsulating fluorescein-labeled cholesterol were prepared as a platform of the imaging agent. Peanut agglutinin (PNA) was immobilized on the surface of fluorescent nanospheres through a chemical reaction with PMAA in order to recognize β-D-galactosyl-(1-3)-*N*-acetyl-D-galactosamine (Gal-β(1-3)GalNAc), which is the terminal sugar of the Thomsen–Friedenreich antigen that is specifically expressed on the mucosal side of colorectal cancer cells. The effect of surface structure of nanospheres on the affinity and specificity of immobilized PNA for Gal-β(1-3)GalNAc was examined. Agglutination of normal and Gal-β(1-3)GalNAc-expressed erythrocytes in the presence of nanospheres showed that PNA was immobilized actively on the nanosphere surface. Molecular weights of PNVA and PMAA affected the PNA activity most strongly. When the weight-average molecular weight of PNVA was nearly equal to that of PMAA, the affinity of PNA immobilized on the nanosphere surface for Gal-β(1-3)GalNAc was as strong as that of intact PNA; the specificity for the carbohydrate residue was higher than that of the PNA. Results indicated that PNVA enhanced the specificity of PNA through the reduction of nonspecific interactions between PNA and carbohydrates other than Gal-β(1-3)GalNAc on the erythrocyte surface without a significant decrease in the affinity.

1. Introduction

Colorectal cancer is a major cause of mortality and morbidity in developed countries [1–3]. Currently, surgical resection is the primary treatment of choice, and early detection and resection are indispensable to cure colorectal cancer [2–5]. Physicians utilize an endoscope to diagnose colorectal cancer definitively although a fecal occult blood testing is popular as the easiest way of screening the cancer [6–8]. This colonoscopy is often accompanied by resection of cancer that remains in the mucous membranes or only minimally invades the submucosal tissues without vessel invasion [9,10]. This minimally invasive operation known as endoscopic mucosal resection (EMR) has several advantages such as low cost, low mortality, and low morbidity and can serve as an alternative to surgical resection [11]. However, a limitation of the current colonoscopy procedure is that it can detect cancers of size more than ca. 1 cm with a relatively high risk of metastasis, although the detectable size depends on the cancer type and the skill of the physician [5,12].

We just started to develop a novel endoscopic imaging agent for the detection of small-sized early colorectal cancer which has few risk of metastasis. Colorectal cancer first develops in the mucous membranes of the large intestine, and invasion and metastasis are observed as the cancer progresses. We noted the mechanism of the cancer development, and designed the colonoscopic imaging agent that can recognize tumor-derived changes in the large intestinal mucosa with high affinity and specificity. The Thomsen–Friedenreich (TF) antigen is specifically expressed on the mucosal side of cancer cells in the early stage of colorectal cancer [13–15]. Its terminal sugar is β-D-galactosyl-(1-3)-*N*-acetyl-D-galactosamine (Gal-β(1-3)GalNAc), and it is masked by oligosaccharide side chain extension or sialylation in normal cells [13–16]. Surface glycoproteins are integral components that act as receptors for different compounds [17–20]. It is known that peanut (*Arachis hypogaea*) agglutinin (PNA) binds to the TF antigen specifically through the recognition of Gal-β(1-3)GalNAc [13,18–21]. Poly(*N*-(2-hydroxypropyl)methacrylamide) (HPMA)–drug conjugates bearing PNA

* Corresponding author. Faculty of Pharmaceutical Sciences, Setsunan University, 45-1, Nagaotoge-cho, Hirakata, Osaka 573-0101, Japan. Tel.: +81 72 866 3124; fax: +81 72 866 3126.
E-mail address: sakuma@pharm.setsunan.ac.jp (S. Sakuma).

0939-6411/$ - see front matter © 2008 Elsevier B.V. All rights reserved.
doi:10.1016/j.ejpb.2008.04.027

have been investigated as anticancer agents for colorectal cancer [22–25]. PNA may be utilized as a targeting moiety of the imaging agent against cancer tissues in the large intestine.

On the other hand, the tumor-derived change in the large intestinal mucosa is a very slight one through the whole large intestine. In order to detect this change accurately, the imaging agent should be designed from the standpoints of not only strong affinity for targets (cancer tissues) but also the minimization of nonspecific interactions with nontargets (normal tissues). Poly(ethylene glycol) (PEG) is well known as a material that reduces the nonspecific interactions through the formation of hydrophilic barriers [26,27]. Chemical bonding of PEG to drugs and drug carriers known as PEGylation are used commercially as a technique that provides long circulation half-lives after intravenous administration. However, Ishida et al. found that anti-PEG IgM elicited by the first dose of PEGylated liposomes mainly initiated the accelerated blood clearance of a subsequent dose of the liposomes [28]. This finding may support that even PEG cannot remove nonspecific interactions completely.

We have been separately investigating core-corona type nanospheres composed of graft copolymers having a hydrophobic polystyrene backbone and hydrophilic polyvinyl branches [29–33]. The size of the nanospheres is adjusted to the magnitude of 10^2 nm, and the hydrophobic polystyrene core is covered with hydrophilic polyvinyl chains. By changing the chemical structure of polyvinyl chains, nanospheres with diverse surface properties can be obtained. Furthermore, macromolecules such as lectins can be immobilized chemically on the surface of nanospheres via a linker such as poly(methacrylic acid) (PMAA) [34]. Hydrophobic and hydrophilic compounds with small molecular weights can be incorporated into the hydrophobic core and onto the hydrophilic corona, respectively, through their physicochemical interactions. The potential of these nanospheres in medical fields is currently being studied [32,34–36]. When the behavior of nanospheres in the gastrointestinal tract was examined, it was found that nanospheres with surface poly(*N*-vinylacetamide) (PNVA) chains rarely interact with the mucous membranes [32,37,38]. This property of PNVA may minimize nonspecific interactions between the imaging agent and normal tissues in the large intestine.

Core-corona type nanospheres with both surface PNVA and PMAA chains can be used as a platform of the imaging agent. Delivery of the imaging agent into cancer tissues appears to be achieved through biorecognition of Gal-β(1-3)GalNAc of the TF antigen by PNA immobilized on the nanosphere surface via the PMAA linker. It is expected that PNVA enhances PNA-induced biorecognition through the reduction of nonspecific interactions between the imaging agent and normal tissues. We propose to use a fluorescent endoscope, which is currently being developed by Olympus Co., Ltd. (a leading manufacturer of endoscopes), to detect the imaging agent accumulated on the surface of cancer tissues visually [39]. Endoscopically detectable fluorescent intensity will be achieved by using a sufficient amount of a hydrophobic fluorescent compound that is strongly encapsulated into the polystyrene core of PNA-immobilized nanospheres with surface PNVA chains.

This is our first report on the colonoscopic imaging agent illustrated in Fig. 1. Here, we succeeded to optimize the surface structure of nanospheres from the standpoint of the maximization of the affinity and specificity of immobilized PNA for Gal-β(1-3)GalNAc.

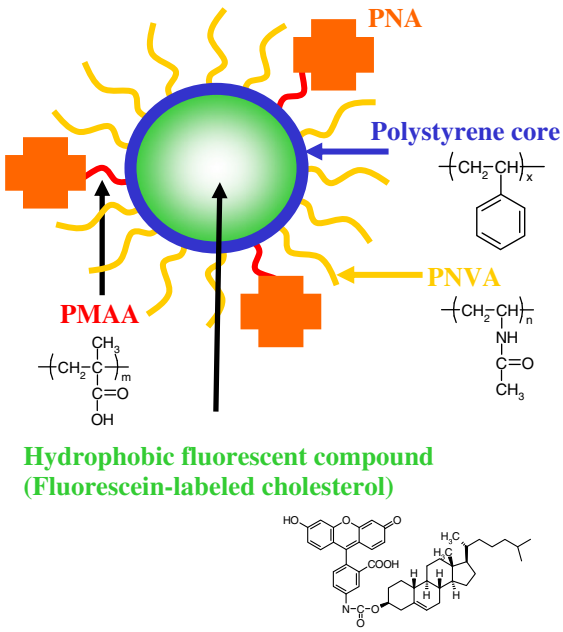

Fig. 1. Schematic representation of PNA-immobilized fluorescent nanospheres with surface PNVA chains.

2. Materials and methods

2.1. Materials

NVA monomers were gifted by Showa Denko Co. (Tokyo, Japan). Fluorescein-5-carbonyl azide diacetate (F-6218) was obtained from Invitrogen Co. (Tokyo, Japan). Tritiated cholesterol (cholesterol [1,2-3H], 1.48–2.22 TBq/mmol, 37 MBq/mL of ethanol) was purchased from Muromachi Yakuhin Co., Ltd. (Tokyo, Japan). All other chemicals were commercial products of reagent grade. Styrene was purified by distillation under reduced pressure, and 2,2′-Azobisisobutyronitrile (AIBN) was purified by recrystallization from acetone. All other chemicals were used without further purification. PNA, *Agaricus bisporus agglutinin* (ABA), and *Artocarpus integrifolia agglutinin* (AIA) were obtained from Sigma–Aldrich (St. Louis, MO, USA). Dulbecco's Phosphate Buffered Saline (product number: D8662, with calcium chloride and magnesium chloride), Dulbecco's Phosphate Buffered Saline, Modified (D8537, without the divalent metal ions), Dulbecco's Modified Eagle's Medium (D5796), and McCOY'S 5A Medium, Modified (M8403) were also obtained from Sigma–Aldrich and used as Phosphate Buffered Saline (PBS). Hereafter, we have used the manufacturer-assigned product number of PBS. Rabbit preserved blood was purchased from Nippon Bio-Test Laboratories Inc. (Tokyo, Japan). Neuraminidase (sialidase, 1 U/mL, extract from *Arthrobacter ureafaciens*) was obtained from Roche Diagnostics (Indianapolis, IN, USA).

2.2. Preparation of PNA-immobilized fluorescent nanospheres with surface PNVA chains (imaging agent)

2.2.1. Preparation of core-corona type nanospheres

Core-corona type nanospheres with surface PNVA and/or PMAA chains were prepared according to the procedure described in our previous studies [32,35]. Briefly, PNVA and poly(*tert*-butyl methacrylate) (PBMA) were prepared by the free radical polymerization of NVA and butyl methacrylate (BMA) monomers, respectively, by using AIBN as an initiator in the presence of 2-mercaptoethanol as a chain transfer agent in ethanol. The resulting hydroxyl group-terminated PNVA and PBMA were reacted with *p*-chloromethyl styrene to introduce a polymerizable vinylbenzyl group in an alkaline solution with tetrabutylphosphonium bromide as a phase transfer catalyst. Vinylbenzyl group-terminated PBMA was hydrolyzed in an acidic solution with hydroquinone as a polymerization inhibitor to obtain vinylbenzyl group-terminated PMAA. Nanospheres, whose chemical structure is shown in Fig. 2, were

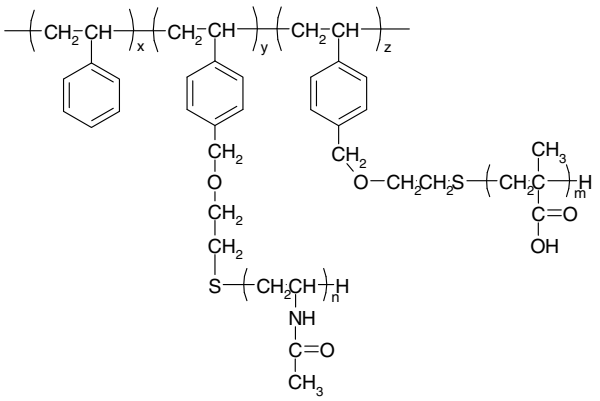

Fig. 2. Chemical structure of core-corona type nanospheres with surface PNVA and PMAA chains.

prepared using a modification of the dispersion copolymerization process described in our previous studies [29–35]. As shown in Table 1, vinylbenzyl group-terminated PNVA, vinylbenzyl group-terminated PMAA, and styrene were weighed in a glass tube and dissolved in 5 mL of ethanol/water mixture (2:1, v/v) containing AIBN (ca. 1 mol% of the total monomers). The solution was bubbled with nitrogen for 30 min, and the tube was then sealed. The copolymerization was successively carried out at 60 °C for 24 h under mild stirring. After centrifugation of the resulting nanosphere dispersion (6200*g*, 15 min), the supernatant containing unreacted substances was removed, and the precipitated nanospheres were dispersed in the ethanol/water mixture. This process was repeated three times. The precipitated nanospheres were finally dispersed in purified water and lyophilized.

2.2.2. Synthesis of fluorescein-labeled cholesterol [40]

Cholesterol (264 mg) and fluorescein-5-carbonyl azide diacetate (10 mg) were weighed in a 25-mL round-shaped flask and dissolved in 4 mL of *N*, *N*-dimethylformamide. After incubation of the solution at 70 °C for 1 h, 2 drops of hydroxylamine aqueous solution (50 w/v%) and 2 mL of ethanol were added and mixed well. Purified water (20 mL) was added and the precipitate was collected by filtration. The filtrate was washed with purified water to remove water-soluble unreacted fluorescein-5-carbonyl azide diacetate and dried under a vacuum. The resulting vivid yellow-colored solid was used without further purification. Gel permeation chromatography (system: HLC-8220GPC, Tosoh, Tokyo, Japan; column: ResiPore, Polymer Laboratories Ltd., Shropshire, UK; mobile phase: THF) showed that the solid contained 6% fluorescein-labeled cholesterol and 94% unreacted cholesterol as impurity.

2.2.3. Encapsulation of fluorescein-labeled cholesterol into core-corona type nanospheres

One hundred milligrams of core-corona type nanospheres were dispersed in 1 mL of ethanol/water mixture (325:175, v/v). In the case of nanospheres with only surface PNVA chains, the ethanol/water mixture was substituted with ethanol. The nanosphere dispersion was mixed with 1 mL of ethanol dissolving 5 mg of fluorescein-labeled cholesterol (5 mg of fluorescein-labeled cholesterol/100 mg of nanospheres). Purified water was dropped into the dispersion under mild stirring until the total volume reached 20 mL. The nanosphere dispersion was centrifuged at 18,400*g* for 15 min (all nanospheres were collected as a precipitate), the supernatant was removed, and the precipitated nanospheres were dispersed in 10 mL of purified water. This process was repeated three times, and the precipitated fluorescent nanospheres were finally dispersed in purified water at a concentration of 20 mg/mL. The dispersion was lyophilized to obtain powdered fluorescent nanospheres.

Separately, in order to estimate encapsulation efficiency of cholesterol, radiolabeled nanospheres were prepared. One milliliter of ethanol dissolving 5 mg of fluorescein-labeled cholesterol was substituted with an equivalent volume of ethanol dissolving 5 mg of cholesterol with 20 μL of tritiated cholesterol ethanol solution. Radiolabeled nanospheres dispersed in purified water at a concentration of 20 mg/mL were obtained by means of the same procedure as described above (the radioactivity of the dispersion was adjusted to ca. 100 kBq/mL). The dispersion and its supernatant (10 μL each) were mixed with 10 mL of scintillation fluid, respectively. After the mixtures were kept at room temperature for 6–12 h, the radioactivity was measured with a liquid scintillation counter (LSC 3500, Aloka, Tokyo, Japan).

2.2.4. Immobilization of PNA on the surface of fluorescent nanospheres

Immobilization of PNA on the nanosphere surface via the PMAA linker was carried out using a modification of the procedure described by Akashi et al [34]. Fifty milligrams of fluorescent nanospheres were dispersed in 10 mL of 0.05 M KH_2PO_4 aqueous solution dissolving 20 mg of 1-ethyl-3-(3-dimetylaminopropyl)-carbodiimide. After incubation of the dispersion at 4 °C for 30 min, the nanospheres with activated carboxyl groups in the PMAA chains were collected by centrifugation (18,400*g*, 15 min). The nanospheres were dispersed in 10 mL of PBS (D8537) dissolving 2.5–10 mg of PNA and incubated at 4 °C for 24 h. The nano-

Table 1
Characterization of core-corona type nanospheres with surface PNVA and/or PMAA chains

Run	In feed [g (mmol)]			Particle size[a] (nm)	Zeta potential (mV)	NVA/MAA[b]
	PNVA[c]	PMAA[d]	Styrene			
1	2.0 (0.40)[e]	0.0 (0.0)	2.0 (19.2)	430 ± 47	−1.6	1/0
2	1.5 (0.30)[e]	0.5 (0.09)[g]	2.0 (19.2)	530 ± 111	−0.3	0.47/0.53
3	1.0 (0.20)[e]	1.0 (0.18)[g]	2.0 (19.2)	450 ± 79	−0.3	0.46/0.54
4	0.5 (0.10)[e]	1.5 (0.27)[g]	2.0 (19.2)	380 ± 52	−3.2	0.29/0.71
5	0.0 (0.0)	2.0 (0.36)[g]	2.0 (19.2)	320 ± 40	−27.8	0/1
6	0.5 (0.13)[f]	0.5 (0.09)[g]	1.0 (0.96)	510 ± 69	−15.4	0.45/0.55
7	0.5 (0.13)[f]	0.5 (0.05)[h]	1.0 (0.96)	580 ± 95	−32.5	0.42/0.58

[a] Weight-average diameter (mean ± s.d.).
[b] Ratio of NVA units to MAA units on the nanosphere surface calculated from ESCA spectra.
[c] Vinylbenzyl group-terminated PNVA.
[d] Vinylbenzyl group-terminated PMAA.
[e] PNVA with weight- and number-average molecular weights (M_w/M_n) of 14,000/5000.
[f] PNVA with M_w/M_n of 9500/4000.
[g] PMAA with M_w/M_n of 10,000/5600.
[h] PMAA with M_w/M_n of 19,000/10,000.

sphere dispersion was centrifuged (18,400*g*, 15 min), the supernatant was removed, and the precipitated nanospheres were dispersed in 10 mL of purified water. This process was repeated three times, and the precipitated PNA-immobilized fluorescent nanospheres with surface PNVA chains (imaging agent) were finally dispersed in purified water at a concentration of 20 mg/mL.

2.3. Characterization

2.3.1. Core-corona type nanospheres with surface PNVA and/or PMAA chains

Core-corona type nanospheres were characterized as described in our previous studies [32,35]. Briefly, weight- and number-average molecular weights (M_w/M_n) of the surface PNVA and PMAA chains were determined by gel permeation chromatography (system: HLC-8220GPC, Tosoh; column: MesoPore (for PNVA) or ResiPore (for PBMA), Polymer Laboratories Ltd.; mobile phase: 0.05 M LiBr (for PNVA) or THF (for PBMA)). Polyethylene glycol and polystyrene (standard samples with known molecular weights) were used to provide calibration curves for PNVA and PBMA, respectively. The value of M_w/M_n of the surface PMAA chains was calculated based on those of PBMA chains. The nanosphere size was measured by dynamic light scattering spectrophotometry with measurement time of 180 s (Honeywell Microtrac UPA, Honeywell International Inc., Morristown, NJ, USA) and scanning electron microphotography (S-3500N, Hitachi Co., Ltd., Tokyo, Japan). The zeta potential of the nanospheres was measured by electrophoretic light scattering spectrophotometry (ELS-800, Otsuka Electronics Co., Osaka, Japan) in PBS (D8537) at 25 °C. The ratio of NVA units to MAA units on the nanosphere surface was evaluated by electron spectroscopy for chemical analysis (ESCA) (Kratos Axis Ultra, Shimadzu Co., Kyoto, Japan).

2.3.2. PNA-immobilized fluorescent nanospheres with surface PNVA chains

Leakage of fluorescein-labeled cholesterol from PNA-immobilized fluorescent nanospheres with surface PNVA chains was evaluated. Nanospheres were dispersed in PBS (D8537, D5796 and M8403) at a concentration of 10 mg/mL and incubated at a rate of 40 strokes/min at 37 °C for 24 h. After centrifugation of the nanosphere dispersion (18,400*g*, 15 min), the absorbance of supernatant was measured at 495 nm by UV–vis spectrophotometry (V-550, JASCO Co., Tokyo, Japan) (average of three experiments). Lower limit of quantification corresponded to 1.0% of fluorescein-labeled cholesterol released from nanospheres.

PNA-immobilized fluorescent nanospheres with surface PNVA chains were dispersed in purified water at an adequate concentration. The fluorescent microphotograph was measured using a fluorescent microscope at an excitation of 470–495 nm and an emission of 510–550 nm (IX71-22FL/PH, Olympus Co., Ltd., Tokyo, Japan).

The amount of PNA immobilized on the nanosphere surface was measured by the ninhydrin method [34]. Ninhydrin (400 mg) and hydrindantin (60 mg) were dissolved in 15 mL of 2-methoxyethanol. The solution was cooled with ice and bubbled with nitrogen for 1 h. After bubbling, 5 mL of acetate-buffered solution (4 M, pH 5.5) was added to prepare the ninhydrin solution. In a separate step, PNA-immobilized fluorescent nanospheres were dispersed in PBS (D8537) at a concentration of 5 mg/mL. One milliliter of the dispersion was mixed with 0.5 mL of 6 M HCl aqueous solution in a glass tube. The tube was sealed and incubated at 100 °C for 2 h. After hydrolytic cleavage of PNA, the nanospheres were removed by filtration, and the filtrate was neutralized by adding an adequate amount of 6 M NaOH aqueous solution. The filtrate containing PNA-derived amino acids was mixed with 0.3 mL of the ninhydrin solution, and the mixture was incubated at 100 °C for 0.5 h. After the reaction, the absorbance was measured at 595 nm by using a microplate reader (Model 3550UV, Bio-Rad Laboratories, Hercules, CA, USA). The calibration curve was prepared by substituting nanospheres with intact PNA. The amount of PNA immobilized on the nanosphere surface was expressed as PNA amount (μg) per milligram of the nanospheres (average of three experiments).

2.4. Biorecognition

The biorecognition of PNA-immobilized fluorescent nanospheres with surface PNVA chains was evaluated using the conventional hemagglutination test [41–43]. Two experiments were carried out for each nanosphere. When there was difference in data between 2 experiments, additional 2 experiments were carried out, and the average of 4 experiments was calculated. Data of intact PNA, which was a control experiment, were expressed as the average of all 8 experiments performed in this study. PBS (D8662) was used because PNA is a C-type lectin that requires calcium ions for carbohydrate binding.

Two milliliters of rabbit preserved blood was mixed with 4 mL of PBS. After centrifugation of the mixture (1000*g*, 30 min), the precipitated erythrocyte fraction was dispersed in 4 mL of PBS. This washing process was repeated three times, and the erythrocytes were finally suspended in PBS at a concentration of 2 v/v%. A portion of the precipitated erythrocyte fraction was mixed with an equivalent volume of neuraminidase solution (1 U/mL), and the mixture was incubated at 37 °C for 1 h. The resulting Gal-β(1-3)GalNAc-expressed erythrocytes were washed with PBS in the same manner as described above, and finally suspended in PBS at a concentration of 2 v/v%. In a separate step, intact PNA was dissolved in PBS at a concentration of 0.25 mg/mL. PNA-immobilized fluorescent nanospheres with surface PNVA chains were also dispersed in PBS, and their concentration was adjusted to 0.25 mg/mL equivalent to that of PNA. A twofold dilution series (50 μL) of both PBS solutions was prepared in a 96-well microtiter U-plate, 50 μL of the erythrocyte suspension was added to each well, and the mixture was incubated at room temperature for 1 h. Agglutination of erythrocytes was observed with a naked eye, and the minimum concentration of PNA in the mixture that induced erythrocyte agglutination was measured. This concentration was defined as the minimum agglutination concentration (MAC). The same test was performed for other intact lectins (ABA and AIA) and core-corona type nanospheres without immobilized PNA ($n = 2$).

A hemagglutination test was also carried out in the presence of carbohydrates ($n = 2$). Galactose or lactose was dissolved in PBS at a concentration of 0.2 M. A twofold dilution series of PNA and PNA-immobilized fluorescent nanospheres with surface PNVA chains (25 μL) was prepared in a 96-well microtiter U-plate. To each well, 25 μL of the carbohydrate solution was added, followed by the addition of 50 μL of the erythrocyte suspension. MAC was measured after 1-h incubation of the mixture at room temperature.

3. Results

3.1. Core-corona type nanospheres with surface PNVA and/or PMAA chains

Table 1 shows the characteristics of core-corona type nanospheres prepared as a platform of the imaging agent. The M_w/M_n values of PNVA were 14,000/5000 and 9500/4000. As shown in our past researches, an increase in the amount of 2-mercaptoethanol resulted in the reduction of the molecular weight of PNVA [32,35]. PMAA with different molecular weights (M_w/M_n: 19,000/10,000 and 10,000/5600), as well as PNVA, were synthe-

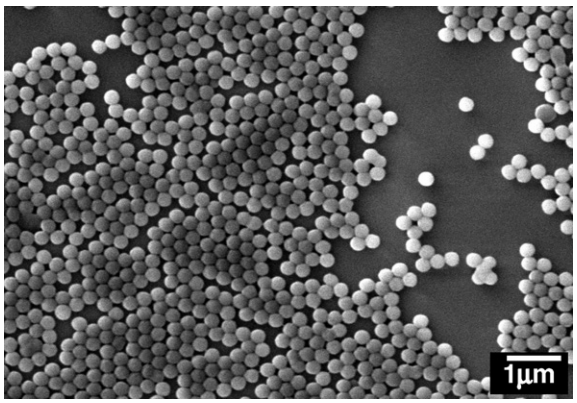

Fig. 3. Scanning electron microphotograph of core-corona type nanospheres with surface PNVA and PMAA chains (Run 3, Table 1).

sized. Seven types of nanospheres (Runs 1–7) were prepared by changing the ratio of vinylbenzyl group-terminated PNVA to vinylbenzyl group-terminated PMAA and the combination of them with different molecular weights in the dispersion copolymerization process. The weight-average diameters of the nanospheres were in the range of approximately 300–600 nm. Chemical composition of the nanospheres did not affect their size clearly. The size distribution of these spherical nanospheres was very narrow as evident in their scanning electron microphotographs. The microphotograph of nanospheres (Run 3) is shown in Fig. 3. The zeta potential of nanospheres with only surface anionic PMAA chains (Run 5) was −27.8 mV in PBS. This negative charge disappeared when nonionic PNVA chains with the molecular weights of 14,000/5000 (M_w/M_n) were introduced on the nanosphere surface, irrespective of the ratio of vinylbenzyl group-terminated PNVA to vinylbenzyl group-terminated PMAA (Runs 2, 3, and 4). However, the negative charge of PMAA remained when the weight-average molecular weight of PNVA was nearly equal to or lower than that of PMAA (Runs 6 and 7). The characteristics of the core-corona type nanospheres were the same as those described in our previous studies [32,35].

When ESCA analysis of nanospheres with only surface PNVA chains (Run 1) was carried out, a PNVA-derived O1s energy peak was observed at 528.2 eV. PMAA-derived O1s energy peaks were observed at 529.2 eV and 531.7 eV when nanospheres with only surface PMAA chains (Run 5) were analyzed. These O1s energy peaks were somewhat overlapped at the above-mentioned three positions in the ESCA spectra of nanospheres with surface PNVA and PMAA chains (Runs 2, 3, 4, 6, and 7). The overlapped peaks were separated mathematically based on the binding energy of NVA and MAA units [44,45]. The ratio of NVA units to MAA units on the nanosphere surface calculated from respective areas of O1s energy peaks was almost consistent with that fed in the reaction, except for Run 2. There was no difference in the ratio between Run 2 and Run 3, even though an excess amount of vinylbenzyl group-terminated PNVA was used for the preparation of Run 2.

3.2. PNA-immobilized fluorescent nanospheres with surface PNVA chains (imaging agent)

Table 2 summarizes the preparation of PNA-immobilized fluorescent nanospheres with surface PNVA chains. Nanospheres with only surface PNVA chains (Run 1) were not used because PNA was immobilized on the nanosphere surface through the coupling of amino groups of PNA with carboxyl groups of PMAA. As shown in Table 2, the amount of immobilized PNA increased with an increase in PNA concentration in the reaction between PNA and fluorescent nanospheres (Runs 2-1, 2-2, and 2-3) and with a decrease in the ratio of NVA units to MAA units (Runs 2-1, 3-1, 4-1, and 5-1). The immobilized amount of PNA did not depend on the molecular weight of PMAA (Runs 3-1, 6-1, and 7-1).

The strength of encapsulation of fluorescein-labeled cholesterol in polystyrene cores of nanospheres was evaluated. Nanospheres encapsulating fluorescein-labeled cholesterol at a concentration of 5 w/w% (Run 2-3) were used. After incubation of the nanospheres at 37 °C for 24 h in PBS, there was no peak at 495 nm which derived from fluorescein-labeled cholesterol in the supernatant. This showed that fluorescein-labeled cholesterol was not released from the nanospheres to any measurable extent. When encapsulation efficiency was examined by using radiolabeled nanospheres with surface PNVA chains (Runs 1 and 3), the efficiency was 98.3% (Run 1) and 100.0% (Run 3). The radioactivity in the supernatant of the resulting radiolabeled nanosphere dispersion was almost the same as that of the background. Mass balance of radiolabeled cholesterol through the preparation process showed that about 70% of applied radiolabeled cholesterol was encapsulated into the nanospheres.

Fig. 4 shows a fluorescent microphotograph of PNA-immobilized fluorescent nanospheres with surface PNVA chains (Run 2-3). Individual nanospheres were clearly observed with a strong fluorescent intensity by using the fluorescent microscope. Fluorescent microscopy indicated that the fluorescent intensity decreased with a decrease in the concentration of fluorescein-labeled cholesterol encapsulated in the nanospheres (data not shown). The absence of vivid yellow color in the background supported the fact that there was no leakage of fluorescein-labeled cholesterol from the nanospheres into the purified water.

3.3. Biorecognition

Lectins are proteins that recognize and bind reversibly to specific carbohydrate residues expressed on the cell surface [18–21].

Table 2
PNA-immobilized fluorescent nanospheres with surface PNVA chains (imaging agents)

Run	Weight- and number-average molecular weights		NVA/MAA[a]	PNA conc.[b] (mg/mL)	Immobilized PNA[c] (μg/mg)
	PNVA (M_w/M_n)	PMAA (M_w/M_n)			
2-1	14,000/5000	10,000/5600	0.47/0.53	1	3.8
2-2	14,000/5000	10,000/5600	0.47/0.53	0.5	2.3
2-3	14,000/5000	10,000/5600	0.47/0.53	0.25	1.5
3-1	14,000/5000	10,000/5600	0.46/0.54	1	3.8
4-1	14,000/5000	10,000/5600	0.29/0.71	1	5.7
5-1	–	10,000/5600	0/1	1	7.0
6-1	9500/4000	10,000/5600	0.45/0.55	1	3.0
7-1	9500/4000	19,000/10,000	0.42/0.58	1	3.1

[a] Ratio of NVA units to MAA units on the nanosphere surface calculated from ESCA spectra.
[b] PNA concentration in the reaction between PNA and fluorescent nanospheres.
[c] Immobilized amount (μg) of PNA per milligram of nanospheres (average of 3 experiments).

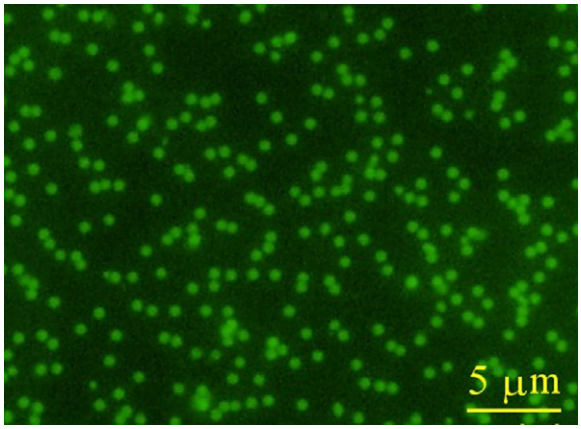

Fig. 4. Fluorescent microphotograph of PNA-immobilized fluorescent nanospheres with surface PNVA chains encapsulating fluorescein-labeled cholesterol at a concentration of 5 w/w% (Run 2-3, Table 2).

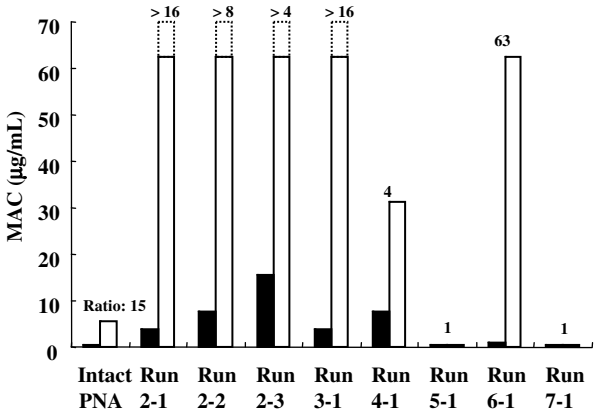

Fig. 5. Erythrocyte agglutination in the presence of PNA-immobilized fluorescent nanospheres with or without surface PNVA chains. MAC was expressed as the minimum concentration of PNA immobilized on the nanosphere surface that induced erythrocyte agglutination (■: MAC for neuraminidase-treated erythrocytes; □: MAC for untreated erythrocytes; Number: ratio of MAC for untreated erythrocytes to MAC for neuraminidase-treated ones). Each bar was expressed as an average of 2 experiments except for Run 6-1 (average of 4 experiments). Run numbers correspond to those in Table 2.

This biorecognition of lectins can be evaluated using the conventional hemagglutination test [41–43]. Since a lectin molecule possesses several sites that bind carbohydrate residues on the erythrocyte surface, a cross-linking network is formed between lectins and erythrocytes, thereby inducing erythrocyte agglutination. MAC—the minimum concentration of lectins that induces erythrocyte agglutination—decreases with an increase in the affinity of lectins for the corresponding carbohydrate residues. The pretreatment of erythrocytes with enzymes such as neuraminidase and trypsin results in the expression of carbohydrate residues that differ from the original residues. Gal-β(1-3)GalNAc is expressed on the surface of neuraminidase-treated erythrocytes. Since PNA, ABA, and AIA are lectins that recognize Gal-β(1-3)GalNAc, their affinity and specificity for this carbohydrate can be estimated by comparing MACs for neuraminidase-treated and untreated erythrocytes. The average MAC of intact PNA was 0.39 and 5.7 μg/mL for neuraminidase-treated and untreated erythrocytes, respectively. The ratio of MAC (MAC for untreated erythrocytes/MAC for neuraminidase-treated erythrocytes) was 15. The affinity and specificity of ABA for Gal-β(1-3)GalNAc were considerably lower than those of PNA (MAC of ABA for neuraminidase-treated erythrocytes: 7.8 μg/mL; MAC of ABA for untreated erythrocytes: 16 μg/mL). The affinity of AIA for Gal-β(1-3)GalNAc was as strong as that of PNA; however, the specificity of AIA was not observed (MAC of AIA for neuraminidase-treated erythrocytes: 0.49 μg/mL; MAC of AIA for untreated erythrocytes: 0.49 μg/mL).

Erythrocyte agglutination by core-corona type nanospheres without immobilized PNA was also examined. Nanospheres with only surface PMAA chains (Run 5) induced erythrocyte agglutination when the concentration of nanospheres was more than 0.00625 mg/mL, irrespective of erythrocyte pretreatment. On the other hand, agglutination of neuraminidase-treated and untreated erythrocytes was not observed even when the concentration of nanospheres with only surface PNVA chains (Run 1) was more than 20 mg/mL, which was the maximum nanosphere concentration used for the evaluation of erythrocyte agglutination due to turbidity.

Fig. 5 shows MAC of PNA-immobilized fluorescent nanospheres with or without PNVA chains. MAC was expressed as the minimum concentration of PNA immobilized on the nanosphere surface that induced erythrocyte agglutination. In the absence of PNVA chains on the nanosphere surface (Run 5-1), the MAC for neuraminidase-treated erythrocytes was 1.0 μg/mL, which was as low as that of intact PNA. However, there was no difference in MAC between neuraminidase-treated and untreated erythrocytes, as observed in the case of core-corona type nanospheres with only surface PMAA chains (Run 5). The introduction of surface PNVA chains contributed to the improvement of specificity, which was not observed in PNA-immobilized fluorescent nanospheres with only surface PMAA chains, except for nanospheres whose weight-average molecular weight of PNVA was half that of PMAA (Run 7-1). The MAC for untreated erythrocytes increased with an increase in the ratio of NVA units to MAA units on the nanosphere surface (Runs 3-1 and 4-1). The MAC for neuraminidase-treated erythrocytes decreased with an increase in the amount of PNA immobilized on the nanosphere surface while MAC for untreated erythrocytes was constantly more than 63 μg/mL, which was maximum concentration in this study due to nanosphere-induced turbidity (Runs 2-1, 2-2, and 2-3). However, the molecular weight was a factor that affected erythrocyte agglutination most strongly (Runs 3-1, 6-1, and 7-1). When there was no difference in weight-average molecular weights between PNVA and PMAA on the nanosphere surface (Run 6-1), the average MAC was 1.0 and 63 μg/mL for neuraminidase-treated and untreated erythrocytes, respectively, indicating that the affinity for Gal-β(1-3)GalNAc was as strong as that of intact PNA; the specificity for the carbohydrate residues was higher than that of the PNA. This high specificity disappeared completely when weight-average molecular weight of PNVA was half that of PMAA (Run 7-1).

Binding of lectins with carbohydrate residues expressed on the cell surface is inhibited competitively by a large amount of carbohydrates having the same chemical structure [17–21]. As summarized in Table 3, the MAC of intact PNA for neuraminidase-treated erythrocytes was 0.39 μg/mL in the absence of carbohydrates, but the MAC increased when galactose or lactose was present. Similar results were obtained when the same test was performed for PNA-immobilized fluorescent nanospheres with surface PNVA chains (Run 3-1, Table 2).

Table 3
MAC (μg/mL) of intact PNA and PNA-immobilized fluorescent nanospheres with surface PNVA chains in the presence of carbohydrates

Carbohydrates	Intact PNA	Nanospheres (Run 3-1)[a]
No additives	0.39	3.9
Galactose	15.6	>62.5
Lactose	62.5	>62.5

[a] Run number corresponds to those in Table 2.

4. Discussion

As shown in Fig. 1, there are three prerequisites for an endoscopic imaging agent. First, the agent must have moieties that recognize cancer tissues in the large intestine. PNA, which recognizes Gal-β(1-3)GalNAc of the TF antigen expressed on the mucosal side of cancer cells in the early stage of colorectal cancer, was selected as the corresponding targeting moiety. PNA possessed stronger affinity and higher specificity for the carbohydrate residue when compared with AIA and ABA.

Second, the agent must have moieties that minimize the nonspecific interactions with the normal tissues of the large intestine. PNVA, which was selected as the moiety that minimizes the nonspecific interactions, is a nonionic polymer with strong hydrophilicity. In our previous study, we demonstrated that core-corona type nanospheres were useful as carriers for oral peptide delivery [32,35,37–38]. Some types of nanospheres enhanced the absorption of salmon calcitonin (sCT) in rats via the gastrointestinal tract. The absorption enhancement was affected by the chemical structure of the hydrophilic polymeric chains. The absorption of sCT was most strongly enhanced by nanospheres with surface poly(*N*-isopropylacrylamide) (PNIPAAm) chains; however, nanospheres with surface PNVA chains did not enhance sCT absorption at all [32]. The adhesion of nanospheres to the intestinal mucosa was related to absorption enhancement [32]. It was considered that the lack of absorption-enhancing function of nanospheres with surface PNVA chains resulted from the strong hydrophilicity of PNVA. Thick water layers that were formed on the nanosphere surface probably prevented the nanospheres from interacting with the mucous membranes in the gastrointestinal tract [32,35,37,38]. As shown in Table 1 and based on our previous report, the negative charge of nanospheres with surface PMAA chains was shielded by the introduction of PNVA chains [35]. Complete shielding effect was observed when the weight-average molecular weight of surface PNVA chains was larger than that of PMAA chains. The interference from PNVA was probably related to the formation of water layers on the nanosphere surface whose thickness depends on the molecular weight. We anticipated that PNVA-reduced nonspecific interactions with normal tissues would enhance PNA-induced biorecognition.

Third, the agent must have a fluorescence intensity that is sufficient for providing a clear fluorescent contrast between cancer and normal tissues under a fluorescent endoscope. We prepared PNA-immobilized fluorescent nanospheres with surface PNVA chains encapsulating fluorescein-labeled cholesterol at a concentration of 1 or 5 w/w%. Nanospheres were first dispersed in ethanol dissolving fluorescein-labeled cholesterol. By gradually decreasing the hydrophobicity of the dispersion medium, fluorescein-labeled cholesterol was encapsulated successively into the polystyrene cores of the nanospheres through their hydrophobic interactions. Encapsulation efficiency and mass balance were examined by substituting fluorescein-labeled cholesterol with radiolabeled cholesterol. Results supported the fact that hydrophobic cholesterol was encapsulated into the hydrophobic polystyrene cores of nanospheres strongly and efficiently. A similar experiment was performed in our past research by using 3-(trifluoromethyl)-3-(*m*-[^{125}I]iodophenyl)diazirine [37]. Mass balance showed that only less than 10% of applied diazirine was encapsulated into the nanospheres, although its encapsulation efficiency was almost 100% and no release of diazirine was observed during 2-h incubation with simulated gastrointestinal fluids and genuine fluids obtained from rats' gastrointestinal tract. The low recovery of diazirine from the dispersion medium through the encapsulation process was probably caused by its relatively low hydrophobicity. Individual PNA-immobilized fluorescent nanospheres encapsulating fluorescein-labeled cholesterol at a concentration of 5 w/w% were observed under the fluorescent microscope although the purity of the cholesterol was 6% (Fig. 4). It is anticipated that the nanospheres are accumulated specifically on the surface of cancer tissues in the large intestine after their intracolonic (enema) administration, and that small-sized early colorectal cancer can be detected through observation of a clear fluorescent contrast between the normal and cancer tissues under a fluorescent endoscope, as illustrated in Fig. 6. Endoscopically detectable fluorescent intensity will be achieved by encapsulating a sufficient amount of fluorescein-labeled compounds. The required amount is still unclear in this study, but the synthesis process of fluorescein-labeled cholesterol should be modified to increase the purity.

The chemical structure and characteristics of core-corona type nanospheres with surface PNVA and/or PMAA chains as a platform of the imaging agent are shown in Figs. 2 and 3 and Table 1, respectively. A research group of Akashi has already reported that the particle size increased with a decrease in molecular weights or concentration of vinylbenzyl group-terminated hydrophilic polymers in the dispersion copolymerization [29–32]. However, there was no obvious effect of vinylbenzyl group-terminated PNVA/vinylbenzyl group-terminated PMAA proportion on the particle size. ESCA analysis indicated that the current preparation method did not yield nanospheres whose NVA units were higher than MAA units. A change in the solvent may be required for the preparation of nanospheres with an excess amount of PNVA chains on their surfaces because the polarity of the solvent also affects the surface composition [29–35]. Table 2 shows that PNA was immobilized on the nanosphere surface. Amino groups of PNA were reacted with carboxyl groups of PMAA although PNVA possibly interfered with the reaction.

A focus on this study is to verify the usefulness of PNVA as a material that reduces nonspecific interactions and to consequently maximize the affinity and specificity of PNA immobilized on the nanosphere surface for Gal-β(1-3)GalNAc. The hemagglutination test was performed to evaluate the activity of immobilized PNA. The effect of PNVA and PMAA chains on erythrocyte agglutination was first examined by using core-corona type nanospheres with surface PNVA or PMAA chains. A large difference was observed in the minimum concentration of nanospheres that induced erythrocyte agglutination. The erythrocyte agglutination in the presence of nanospheres with surface PMAA chains was probably caused by PMAA-induced strong nonspecific interactions. Nanospheres with surface PNVA chains did not agglutinate erythrocytes in the range of nanosphere concentration examined in this study. These results indicated that PNVA enabled the imaging agents to reduce nonspecific interactions. As shown in

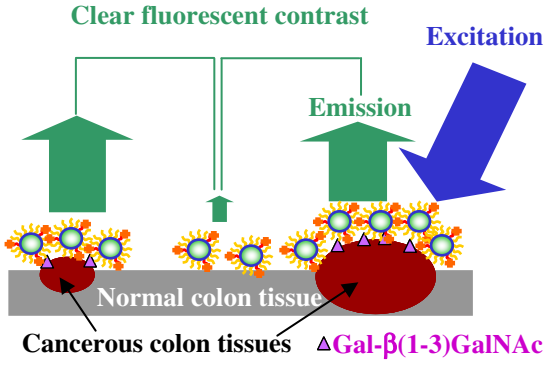

Fig. 6. Principle of the detection of early colorectal cancer by using PNA-immobilized fluorescent nanospheres with surface PNVA chains under the fluorescent endoscope.

Fig. 5, the hemagglutination of neuraminidase-treated erythrocytes was observed in the presence of a small amount of PNA-immobilized fluorescent nanospheres without surface PNVA chains (Run 5-1). However, the specificity was not observed, differing from the case of intact PNA. Erythrocyte agglutination was probably induced by nonspecific interactions occurring due to residual PMAA that had not reacted with PNA. PNVA prevented erythrocyte agglutination caused by PMAA-induced strong nonspecific interactions although this effect was not observed when the molecular weight of PMAA was considerably larger than that of PNVA (Run 7-1). Table 3 indicated that PNA on the nanosphere surface recognized Gal-β(1-3)GalNAc which was expressed on the surface of neuraminidase-treated erythrocytes. The molecular weights of surface PNVA and PMAA chains affected the affinity and specificity of PNA most strongly although the PNA activity was also influenced by the immobilized amount of PNA and the ratio of NVA units to MAA units. When the weight-average molecular weight of PNVA was nearly equal to that of PMAA (Run 6-1), the affinity of PNA immobilized on the nanosphere surface for Gal-β(1-3)GalNAc was as strong as that of intact PNA; the specificity for the carbohydrate residue was higher than that of the PNA. This result indicated that PNVA enhanced the specificity of PNA through the reduction of nonspecific interactions between PNA and carbohydrates other than Gal-β(1-3)GalNAc without a significant decrease in the affinity.

PNA was immobilized actively on the surface of nanospheres, and its biorecognition was enhanced through the surface PNVA-reduced nonspecific interactions between the nanospheres and nontargets. Current data, however, remain to optimize the surface structure of nanospheres using the hemagglutination test. We should first examine biorecognition of PNA-immobilized fluorescent nanospheres with surface PNVA chains against human colorectal cancer cells with the TF antigen. In vivo experiments using animals bearing the TF antigen-expressing cancer cells in the large intestinal mucosa will be performed to evaluate the usefulness of the imaging agent practically. The effect of PNVA should be also compared with that of PEG. In the field of imaging agents, PEGylation is being studied for polymeric micelles composed of block copolymers that bound gadolinium ions providing high contrasts in Magnetic Resonance Imaging (MRI) [46]. Studies on these issues will be successively discussed in future reports.

5. Conclusions

PNA-immobilized fluorescent nanospheres with surface PNVA chains were designed with the aim of developing an endoscopic imaging agent for the detection of early colorectal cancer. PNA was actively immobilized on the nanosphere surface and its affinity for Gal-β(1-3)GalNAc, which is the terminal sugar of the TF antigen that is specifically expressed on the mucosal side of colorectal cancer cells, was as strong as that of intact PNA. PNVA enhanced the specificity of PNA for the carbohydrate residue through the reduction of nonspecific interactions between nanospheres and nontargets.

Acknowledgements

This work was financially supported in part by a Grant-in-Aid for scientific research (No. 18590160) from the Ministry of Education, Culture, Sports, Sciences and Technology of Japan (MEXT), a Grant-in-Aid from JFE (The Japanese Foundation for Research and Promotion of Endoscopy), and a Grant-in-Aid from JIST (Japan Interaction in Science & Technology Forum). The authors thank Showa Denko Co. for the gift of NVA monomers.

References

[1] S.L. Parker, T. Tong, S. Bolden, P.A. Wingo, Cancer statistics, CA Cancer J. Clin. 47 (1) (1997) 5–27.
[2] A. Jemal, R. Siegel, E. Ward, T. Murray, J. Xu, C. Smigal, M.J. Thun, Cancer statistics, CA Cancer J. Clin. 56 (2) (2006) 106–130.
[3] http://www.cancer.gov.
[4] G.C. Balch, A. De Meo, J.G. Guillem, Modern management of rectal cancer: a 2006 update, World J. Gastroenterol. 12 (2006) 3186–3195.
[5] T. Muto, M. Oya, Recent advances in diagnosis and treatment of colorectal T1 carcinoma, Dis. Colon Rectum 46 (10 Suppl.) (2003) S89–S93.
[6] S.H. Sial, M.F. Catalano, Gastrointestinal tract cancer in the elderly, Gastroenterol. Clin. North Am. 30 (2) (2001) 565–590.
[7] W.V. Harford, Colorectal cancer screening and surveillance, Surg. Oncol. Clin. N. Am. 15 (1) (2006) 1–20.
[8] D. Lieberman, Screening for colorectal cancer in average-risk populations, Am. J. Med. 119 (9) (2006) 728–735.
[9] T. Ponchon, Endoscopic mucosal resection, J. Clin. Gastroenterol. 32 (1) (2001) 6–10.
[10] S. Kudo, Y. Tamegai, H. Yamano, Y. Imai, E. Kogure, H. Kashida, Endoscopic mucosal resection of the colon: the Japanese technique, Gastrointest. Endosc. Clin. N. Am. 11 (3) (2001) 519–535.
[11] B. Rembacken, T. Fujii, H. Kondo, The recognition and endoscopic treatment of early gastric and colonic cancer, Best Prac. Res. Clin. Gastroenterol. 15 (2) (2001) 317–336.
[12] H. Kashida, S. Kudo, Early colorectal cancer: concept, diagnosis, and management, Inter. J. Clin. Oncol. 11 (1) (2006) 1–8.
[13] C.R. Boland, J.A. Roberts, Quantitation of lectin binding sites in human colon mucins by use of peanut and wheat germ agglutinin, J. Histochem. Cytochem. 36 (10) (1988) 1305–1307.
[14] B.J. Campbell, I.A. Finnie, E.F. Hounsell, J.M. Rhodes, Direct demonstration of increased expression of Thomsen–Friedenreich (TF) antigen from colonic adenocarcinoma and ulcerative colitis mucin and its concealment in normal mucin, J. Clin. Invest. 95 (2) (1995) 571–576.
[15] R. Singh, B.J. Campbell, L.-G. Yu, D.G. Fernig, J.D. Milton, R.A. Goodlad, A.J. FitzGerald, J.M. Rhodes, Cell surface-expressed Thomsen–Friedenreich antigen in colon cancer is predominantly carried on high molecular weight splice variants of CD44, Glycobiology 11 (7) (2001) 587–592.
[16] E. Dabelsteen, Cell surface carbohydrates as prognostic markers in human carcinomas, J. Pathol. 179 (4) (1996) 358–369.
[17] A.P. Corfield, B.F. Warren, Mucus glycoproteins and their disease in colorectal disease, J. Pathol. 180 (1) (1996) 8–17.
[18] M.A. Clark, B.H. Hirst, M.A. Jepson, Lectin-mediated mucosal delivery of drugs and microparticles, Adv. Drug Deliv. Rev. 43 (2–3) (2000) 207–223.
[19] C. Bies, C.-M. Lehr, J.F. Woodley, Lectin-mediated drug targeting: history and applications, Adv. Drug Deliv. Rev. 56 (4) (2004) 425–435.
[20] F. Gabor, E. Bogner, A. Weissenboeck, M. Wirth, The lectin-cell interaction and its implications to intestinal lectin-mediated drug delivery, Adv. Drug Deliv. Rev. 56 (4) (2004) 459–480.
[21] J.M. Rini, Lectin structure, Annu. Rev. Biophys. Biomol. Struct. 24 (1995) 551–577.
[22] S. Wróblewski, P. Kopečková, B. Říhová, J. Kopeček, Lectin-HPMA copolymer conjugates: potential oral drug carriers for targeting diseased tissues, Macromol. Chem. Phys. 199 (11) (1998) 2601–2608.
[23] S. Wróblewski, M. Berenson, P. Kopečková, J. Kopeček, Biorecognition of HPMA copolymer–lectin conjugates as an indicator of differentiation of cell-surface glycoproteins in development, maturation, and diseases of human and rodent gastrointestinal tissues, J. Biomed. Mater. Res. 51 (3) (2000) 329–342.
[24] S. Wróblewski, M. Berenson, P. Kopečková, J. Kopeček, Potential of lectin-*N*-(2-hydroxypropyl)methacrylamide copolymer–drug conjugates for the treatment of pre-cancerous conditions, J. Control. Release 74 (1-3) (2001) 283–293.
[25] S. Sakuma, Z.-R. Lu, P. Kopečková, J. Kopeček, Biorecognizable HPMA copolymer–drug conjugates for colon-specific delivery of 9-aminocamptothecin, J. Control. Release 75 (3) (2001) 365–379.
[26] D. Papahadjopoulos, T.M. Allen, G. Gabizon, E. Mayhew, K. Matthay, S.K. Huang, K.D. Lee, M.C. Woodle, D.D. Lasic, C. Redemann, F.J. Martin, Sterically stabilized liposomes: improvements in pharmacokinetics and antitumor therapeutic efficacy, Proc. Natl. Acad. Sci. USA 88 (24) (1991) 11460–11464.
[27] K. Maruyama, O. Ishida, S. Kasaoka, T. Takizawa, N. Utoguchi, A. Shinohara, M. Chiba, H. Kobayashi, M. Eriguchi, H. Yanagie, Intracellular targeting of sodium mercaptoundecahydrododecaborate (BSH) to solid tumors by transferrin-PEG liposomes, for boron neutron-capture therapy (BNCT), J. Control. Release 98 (2) (2004) 195–207.
[28] T. Ishida, S. Kashima, H. Kiwada, The contribution of phagocytic activity of liver macrophages to the accelerated blood clearance (ABC) phenomenon of PEGylated liposomes in rats, J. Control. Release 126 (2) (2008) 162–165.
[29] M. Riza, S. Tokura, M. Iwasaki, E. Yashima, A. Kishida, M. Akashi, Graft copolymers having hydrophobic backbone and hydrophilic branches, X. Preparation and properties of water-dispersible polyanionic microspheres having poly(methacrylic acid) branches on their surfaces, J. Polym. Sci. Polym. Chem. 33 (8) (1995) 1219–1225.
[30] T. Uchida, T. Serizawa, M. Akashi, Graft copolymers having hydrophobic backbone and hydrophilic branches XXI. Preparation of galactose surface-accumulated polystyrene nanospheres and their interaction with lectin, Polym. J. 31 (11_1) (1999) 970–973.

[31] M.-Q. Chen, A. Kishida, T. Serizawa, M. Akashi, Nanospheres formation in copolymerization of methacrylate with poly (ethylene glycol) macromonomers, J. Polym. Sci.; Part A: Polym. Chem. 38 (10) (2000) 1811–1817.
[32] S. Sakuma, M. Hayashi, M. Akashi, Design of nanoparticles composed of graft copolymers for oral peptide delivery, Adv. Drug Deliv. Rev. 47 (1) (2001) 21–37.
[33] M.-Q. Chen, T. Serizawa, M. Li, C. Wu, M. Akashi, Thermosensitive behavior of poly(*N*-isopropylacrylamide) grafted polystyrene nanoparticles, Polym. J. 35 (12) (2003) 901–910.
[34] M. Akashi, T. Niikawa, T. Serizawa, T. Hayakawa, M. Baba, Capture of HIV-1 gp120 and virions by lectin-immobilized polystyrene nanospheres, Bioconjug. Chem. 9 (1) (1998) 50–53.
[35] S. Sakuma, N. Suzuki, R. Sudo, K. Hiwatari, A. Kishida, M. Akashi, Optimized chemical structure of nanoparticles as carriers for oral delivery of salmon calcitonin, Int. J. Pharm. 239 (1–2) (2002) 185–195.
[36] T. Akagi, M. Ueno, K. Hiraishi, M. Baba, M. Akashi, AIDS vaccine: intranasal immunization using inactivated HIV-1-capturing core-corona type polymeric nanospheres, J. Control. Release 109 (1–3) (2005) 49–61.
[37] S. Sakuma, R. Sudo, N. Suzuki, H. Kikuchi, M. Akashi, M. Hayashi, Mucoadhesion of polystyrene nanoparticles having surface hydrophilic polymeric chains in the gastrointestinal tract, Int. J. Pharm. 177 (2) (1999) 161–172.
[38] S. Sakuma, R. Sudo, N. Suzuki, H. Kikuchi, M. Akashi, Y. Ishida, M. Hayashi, Behavior of mucoadhesive nanoparticles having hydrophilic polymeric chains in the intestine, J. Control. Release 81 (3) (2002) 281–290.
[39] Y. Sano, M. Muto, H. Tajiri, A. Ohtsu, S. Yoshida, Optical/digital chemoendoscopy during colonoscopy using narrow-band imaging system, Digestive Endoscopy 17 (Suppl.) (2005) S43–S48.
[40] http://probes.invitrogen.com/handbook/sections/0301.html.
[41] J. Samuel, A.A. Noujaim, G.D. MacLean, M.R. Suresh, B.M. Longenecker, Analysis of human tumor associated Thomsen–Friedenreich antigen, Cancer Res. 50 (15) (1990) 4801–4808.
[42] A. Ikuta, N. Mizuta, S. Kitahara, T. Murata, T. Usui, K. Koizumi, T. Tanimoto, Preparation and characterization of novel branched β-cyclodextrins having β-D-galactose residues on the non-reducing terminal of the side chains and their specific interactions with peanut (*Arachis hypogaea*) agglutinin, Chem. Pharm. Bull. 52 (1) (2004) 51–56.
[43] T. Saito, M. Hatada, S. Iwanaga, S. Kawabata, A newly identical horseshoe lectin with binding specificity to *O*-antigen of bacterial Lipopolysaccharides, J. Bio. Soc. 272 (49) (1997) 30703–30708.
[44] I. Gouzman, M. Dubey, M.D. Carolus, J. Schwartz, S.L. Bernasek, Monolayer vs. multilayer self-assembled alkylphosphonate films: X-ray photoelectron spectroscopy studies, Surf. Sci. 600 (4) (2006) 773–781.
[45] A.C. Rastogi, S.B. Desu, Thermal chemical vapor deposition of fluorocarbon polymer thin films in a hot filament reactor, Polymer 46 (10) (2005) 3440–3451.
[46] E. Nakamura, K. Makino, T. Okano, T. Yamamoto, M. Yokoyama, A polymeric micelle MRI contrast agent with changeable relaxivity, J. Control. Release 114 (3) (2006) 325–333.